

Electrochemical synthesis of 4-aminobenzoic acid from 4-nitrobenzoic acid: fundamental aspects*

F. LAPICQUE, A. STORCK

Laboratoire des Sciences du Génie Chimique, CNRS-ENSIC, 1 rue Grandville, 54042 Nancy Cedex, France

Received 5 February 1986; revised 24 March 1986

On the basis of the electrolytic reduction of 4-nitrobenzoic acid to 4-aminobenzoic acid, the present paper deals with electrochemical engineering in a multi-phase medium. From experimental data a reactor adapted to the electrolytic reduction in a solid-liquid dispersion was designed.

The performances of the reactor are demonstrated in terms of mass transfer towards the electrode and productivity of batch operations. In spite of a fairly good faradaic yield of around 75%, large decays of current density have been observed. Interpretations of this phenomenon, involving limitation by the solubilization of the solid substrate and a possible alteration of the electrode, are presented in the discussion.

Nomenclature

a_e	interfacial electrode area, m^{-1}	l	suspended particle, $m s^{-1}$
A_e	electrode area, m^2	LD	wire broadness, m
a_s	interfacial area of suspended solid, m^{-1}		dimension of expanded metal (long diagonal), m
A_s	suspended solid area, m^2	m	amount of substrate introduced, g
C	bulk concentration of substrate, $mol m^{-3}$ or M	N	stirring rate, r.p.s.
C^*	saturation concentration of substrate, $mol m^{-3}$ or M	P	specific power, $W kg^{-1}$
CD	dimension of expanded metal (short diagonal), m	Q	charge passed, $A s$
d	impeller diameter, m	Q_{max}	maximal charge allowing total conversion of substrate assuming a faradaic yield of 100%, $A s$
D	diffusion coefficient, $m^2 s^{-1}$	Re	Reynolds number = Nd^2/ν
D_c	diameter of the cathodic compartment, m	Sc	Schmidt number = ν/D
e	metal sheet thickness, m	Sh	Sherwood number = $k_d d/D$
F	Faraday's constant	t	time, s
i	current density, $A m^{-2}$	T	temperature, $^{\circ}C$
k_d	mass transfer coefficient at the electrode, $m s^{-1}$	V_c	volume of the cathodic compartment, m^3
k_L	mass transfer coefficient at a solid	x	mole fraction of PABA produced
		α	parameter, defined as $k_d a_e / (k_d a_e + k_L a_s)$
		ν	kinematic viscosity, $m^2 s^{-1}$
		ν_e	number of electrons

1. Introduction

The compound 4-aminobenzoic acid (PABA) is an intermediate in the preparation of dye stuffs

or pharmaceutical substances. It is mainly produced by the reduction of 4-nitrobenzoic acid (PNBA) by catalytic hydrogenation, which has displaced the other chemical routes. Chemical

* This paper was presented at the meeting on 'Electroorganic Process Engineering' held in Perpignan, France, 19-20 September 1985.

methods involve the tedious process of separating PABA from the inorganic agent employed for the reduction. An electrochemical process offers the advantage of giving a product which can be easily isolated in pure form. In the present case the electrochemical reduction takes place in a solid-liquid suspension of slightly solubilized PNBA in an aqueous electrolyte.

In addition to its economic interest, electrochemical reduction represents a good example of electro-organic synthesis allowing the study of phenomena frequently encountered in electrochemical engineering such as reaction in solid liquid suspension and complex kinetics. Previous studies [1-3] dealing with this process mention good performance, i.e. high selectivity and current densities in rather simple electrolyzers, but very few fundamental aspects were examined.

This paper presents a fundamental investigation which makes it possible to propose an efficient electrochemical reactor for the preparation of PABA with the help of the chemical engineering methodology. After reporting the results of preliminary experimental studies, the performance of a reactor adapted to electrochemical reduction are described in terms of several aspects, i.e. mass transfer at the electrode, current density and extent of reaction. In addition, the interpretation of some of the phenomena encountered is proposed.

2. Preliminary studies

Similar to the reduction of nitro compounds, the reaction considered here involves the consumption of H^+ and has to be performed in acid medium. Besides the presence of H^+ , the space time yield of the electrochemical process is directly controlled by the concentration of solubilized nitrobenzoic acid. Numerous measurements of its solubility have been made by means of a UV detector set to 275 nm. It can be seen that the poor solubility of PNBA (below 10^{-2} M) has a weak dependence on acid concentration in the range 1-8 N. In addition, it is found to be an increasing function of temperature (Fig. 1).

The variation of the kinematic viscosity of the acid solution with temperature has been measured and in the case of a 3-M sulphuric medium this variation can be expressed as

$$\nu = 2.096 \times 10^{-6} \exp(-0.0199T) \quad (1)$$

where ν is in $m^2 s^{-1}$ and T in $^{\circ}C$.

The feasibility of the reduction was studied by means of polarographic techniques. Polarograms obtained in an aqueous sulphuric medium (3 M) indicate that the overall reduction involving six electrons can be performed at low cathodic potential (Fig. 2). Furthermore, these curves exhibit two waves with a relative height in the ratio 2:1. Thus, in agreement with Chandra *et al.* [4], this

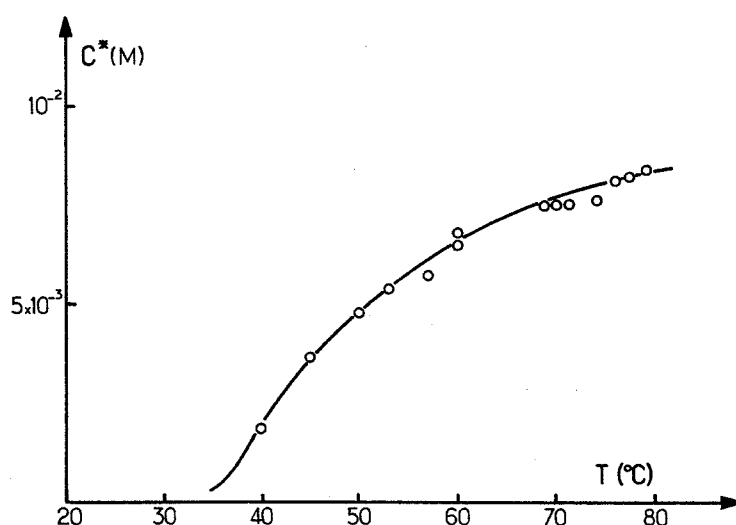


Fig. 1. Variation of PNBA solubility with temperature in a 3 M sulphuric acid medium.

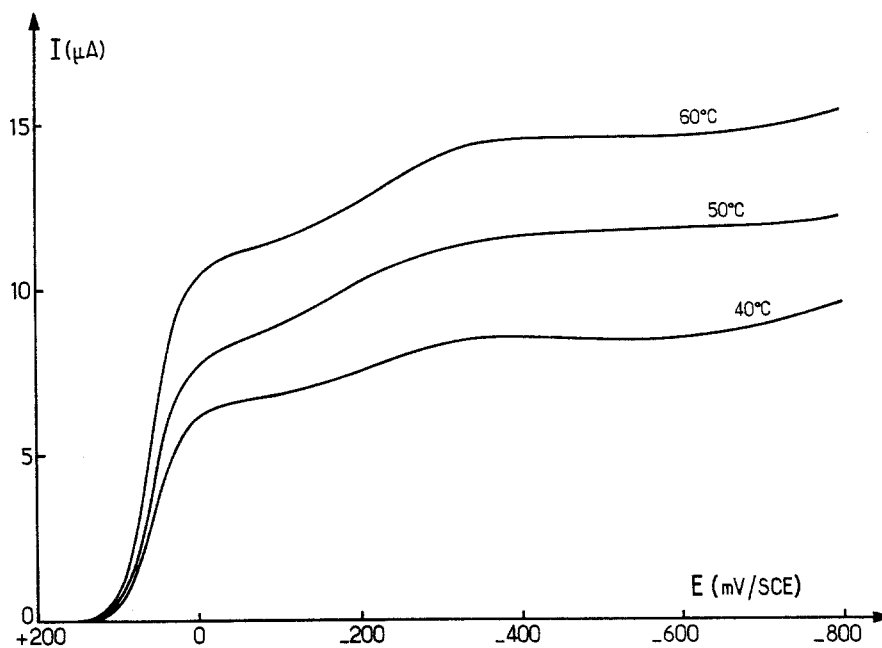


Fig. 2. Polarographic curves of the reduction of PNBA in a 3 M sulphuric acid medium at various temperatures.

indicates the existence of 4-hydroxylamine benzoic acid as an intermediate product obtained through a first reduction involving four electrons.

The diffusion coefficient of PNBA was determined from the polarograms by Ilkovic's equation. Its variation with temperature in a 3-M sulphuric solution is reported in Table 1. The relatively large values of the diffusion coefficient coupled with the amount of solubilized PNBA over 50°C suggest the possibility of obtaining current densities up to 500 A m⁻² in very turbulent conditions.

The results of preliminary experiments suggest that the electro-organic synthesis of PABA could be carried out in a stirred reactor giving both the suspension of PNBA particles and large values of mass transfer coefficients at the cathode.

Table 1. Values of the PNBA diffusion coefficient (D) for various temperatures; 10^{-3} PNBA in aqueous 3 M H_2SO_4

Temperature (°C)	D ($10^{-10} m^2 s^{-1}$)
30	8.0
40	9.6
50	13.1
60	16.5
70	20.7

3. Stirred electrochemical reactor

3.1. Description of the reactor

A laboratory-scale cell was built taking into account the different technological constraints, i.e. suspension of solid, high temperature and corrosive medium.

The cell was a Pyrex glass reactor with a total volume close to 600 cm³ ($6 \times 10^{-4} m^3$) divided into two concentric compartments separated by a Nafion membrane (Fig. 3). The counter electrode, the anode in the present case, was a 500-cm² ($5 \times 10^{-2} m^2$) sheet of expanded platinumized titanium surrounding the membrane. The cathodic compartment inside the anodic zone was designed in the same way as a stirred vessel; its volume was 450 cm³ ($4.5 \times 10^{-4} m^3$) and the diameter D_c of the cylindrical part was $8.0 \times 10^{-2} m$ (Fig. 3). A PTFE impeller (diameter $4.2 \times 10^{-2} m$) was located at the centre of the reactor.

The working electrode was a cylindrical grid of amalgamated copper and several sizes of electrode were considered. The wire netting forming the working electrode had the following dimensions: wire diameter $0.7 \times 10^{-3} m$ for a $2.7 \times 10^{-3} m$ large mesh. The wetted areas of

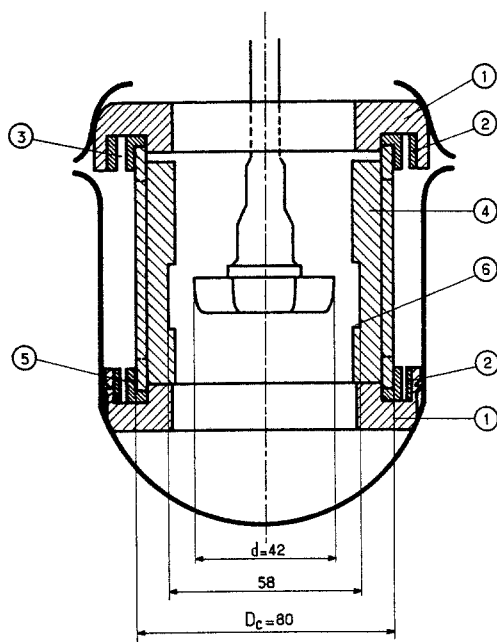


Fig. 3. Schematic view of the reactor (dimensions in mm). 1, Upper and lower fitting crowns; 2, rings; 3, counter electrode bedding; 4, baffles; 5, membrane ring; 6, working electrode bedding.

the grids could be estimated by taking into account the characteristics of the netting and the external dimensions of the electrodes. The area of the electrodes was between 50 and $130 \times 10^{-4} \text{ m}^2$. The grid around the impeller was fixed onto four baffles allowing a turbulent regime throughout the compartment; the electrode was thus perpendicular to the direction of the liquid flow. Voltametric studies were made with a Luggin capillary connected to an external reference electrode.

3.2. Mass transfer in single phase medium

Intrinsic performances of the stirred reactor were first studied in terms of mass transfer coefficient in a homogeneous medium. Mass transfer performance was investigated by the electrochemical reduction of ferricyanide ions. For this part of the work the membrane was removed and the working electrode was a cylindrical sheet of expanded platinized titanium ($17 \times 1.7 \text{ cm}^2$). In order to observe the influence of the geometry of the expanded metal on mass transfer under

Table 2. Characteristics of the meshes in the three types of expanded metal

Mesh type	LD (10^{-3} m)	CD (10^{-3} m)	e (10^{-3} m)	l (10^{-3} m)
1	2.2	1.43	0.25	0.06
2	8.0	3.3	0.40	1.0
3	10.8	6.0	0.85	1.2

our experimental conditions, three different meshes of titanium were used. The characteristic dimensions of the meshes are reported in Table 2. The 'real' or wetted area of such an electrode, denoted A_e , can be determined from the external dimensions of the sheet and geometric calculations with an accuracy of about 5%.

The electrolytic medium had the following chemical composition: potassium ferricyanide, $5 \times 10^{-3} \text{ M}$; potassium ferrocyanide, 0.1 M ; and sodium hydroxyde, 0.5 M . Experimental values obtained at room temperature for the electrolyte kinematic viscosity, ν , the ferricyanide diffusion coefficient, D , and the Schmidt number, Sc , are $0.9 \times 10^{-6} \text{ m}^2 \text{ s}^{-1}$, $8.8 \times 10^{-10} \text{ m}^2 \text{ s}^{-1}$ and 1040, respectively.

The mass transfer coefficients measured in the alkaline solution for the reactor considered in this study are plotted versus the stirring rate, N , in Fig. 4a. The influence of the geometry of the mesh for metals used here seems to be negligible and experimental results can be expressed by the following:

$$k_d = 1.24 \times 10^{-5} N^{0.67} \quad (2)$$

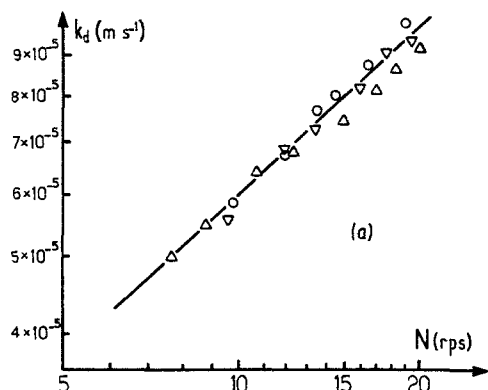
As mass transfer at the electrode is not affected by the mesh geometry, dimensionless parameters such as the Reynolds and the Sherwood numbers can be defined in a similar way as they are defined for stirred vessels [5, 6]:

$$Re = Nd^2/\nu \quad \text{and} \quad Sh = k_d d/D$$

Then Equation 2 may be expressed in the dimensionless form

$$ShSc^{-\frac{1}{3}} = 0.402 Re^{0.664} \quad (3)$$

Furthermore, in a similar way to previous studies [7], mass transfer performance can be roughly interpreted by a macroscopic approach



$$P = 4.4 \times 10^{-4} N^{2.93} \quad (4)$$

Experimental mass transfer results can be described by an energy correlation with the dimensionless group (Pd^4/v^3)

$$ShSc^{-1/3} = 0.346(Pd^4/v^3)^{0.238} \quad (5)$$

Such a correlation can be compared with previous general studies on energetic aspects of turbulent media [8, 9]. For instance, Calderbank and Moo Young [8] proposed the expression

$$ShSc^{-1/3} = 0.13(Pd^4/v^3)^{0.25} \quad (6)$$

and the results of Storck and Hutin [9] are as follows

$$ShSc^{-1/3} = 0.343(Pd^4/v^3)^{0.217} \quad (7)$$

The value of the exponent in P obtained from our experimental results is in good agreement with a corresponding one from Equations 6 and 7; in addition these exponents are very close to the theoretical value of 2/9 expected from dimensional analysis for turbulent flows [7]. However, a comparison of Equations 5, 6 and 7 indicates a certain discrepancy (Fig. 5), as measured mass transfer performance seems to be 70% higher than values expected from the literature correlations. The deviation is probably due to the position of the electrode which faces the impeller. Furthermore, measured values of P correspond to power averaged over the whole reactor; other studies [7] have reported a sharp increase in the vicinity of the impeller due to the corresponding increase of the fluid velocity.

4. Electrochemical reduction

Voltametric curves obtained in the reactor exhibited a large plateau corresponding to a diffusional limitation between -400 and -800 mV. Production experiments were carried out in the batch reactor at -600 mV vs SCE.

The cathode was renewed before each run presented here; the working electrode was carefully washed with a diluted nitric acid solution and then amalgamated by simple contact in a mercury pool for 1 h. During the heating up period in the reactor (~ 2 h) the cathode was maintained at -700 mV vs SCE. The electric supply was

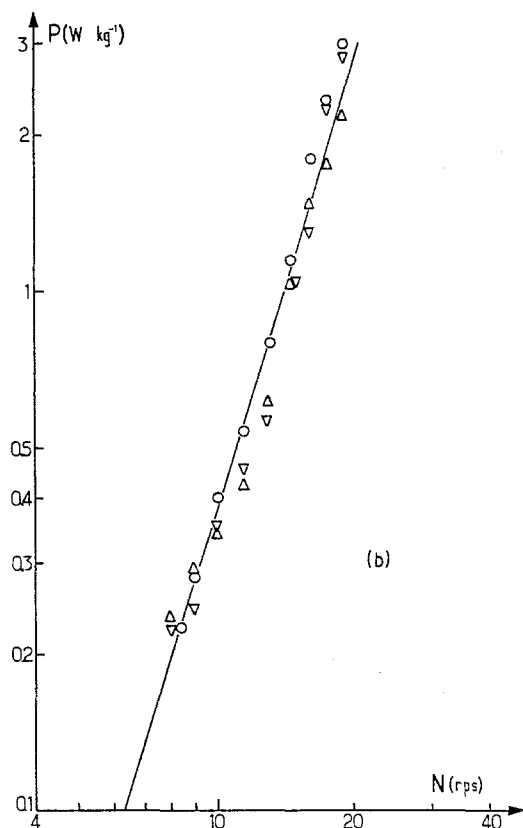


Fig. 4. Mass transfer coefficient (a) and specific power (b) with stirring rate in the reactor. Reduction of potassium ferricyanide at various expanded electrodes (see Table 2). \circ , type 1; ∇ , type 2; \triangle , type 3.

based on the specific power P (per unit mass of fluid). Values of the specific power measured under similar conditions are reported in Fig. 4b and are correlated with N as follows

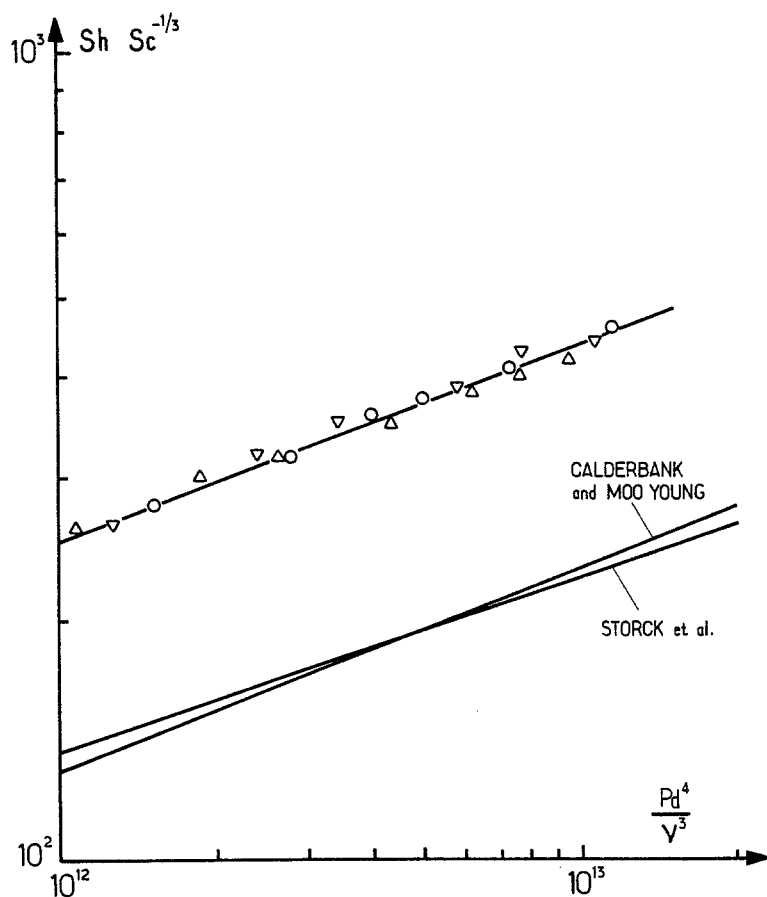


Fig. 5. Variations of mass transfer coefficients expressed as $ShSc^{-1/3}$ with a dimensionless criterion of specific power in the reactor: experimental results and literature data.

switched off as PNBA was introduced into the stirred inner compartment. PNBA (Fluka, purity > 99%) consisted of a coarse powder which has no characteristic shape and exhibits a large size distribution (10^{-4} to 5×10^{-4} m). After a period of 1 h, allowing the saturation of the cathodic bulk with PNBA, the electrochemical operation was started. Current evolution was continuously recorded and the extent of reaction was followed by regular sampling of the bulk accompanied by chemical analysis by TLC. The charge passed was calculated by numerical integration of the recorded current.

The influence of several factors were investigated: the temperature T (60°C or 70°C), the electrode area A_e , and m , the amount of solid PNBA introduced. Stirring rate was arbitrarily fixed at 12 r.p.s. for every trial. If the solubility of the organic substrate and the volume of the catholyte is taken into account, about 0.5 g PNBA was dissolved in the bulk and most experi-

ments were conducted in the presence of a solid suspension of substrate.

4.1. Variation of current density with time

Current density increases with temperature due to the increased solubility of PNBA and the large reduction in the value of the Schmidt number.

In the very early stages of the electrochemical operation, whatever the bulk temperature, a decay of current density is observed (Fig. 6). It can be seen that current density measured at $t = 0$ seems to be mainly influenced by the bulk temperature as it varies between 350 A m^{-2} at 60°C and 500 A m^{-2} at 70°C . In contrast, the decay is controlled by the amount of PNBA introduced and the electrode area.

For small values of m (0.5 g, 1 g) this decrease is a very important phenomenon and occurs throughout the experiment. The dotted curve shows the variation of i with time, taking into

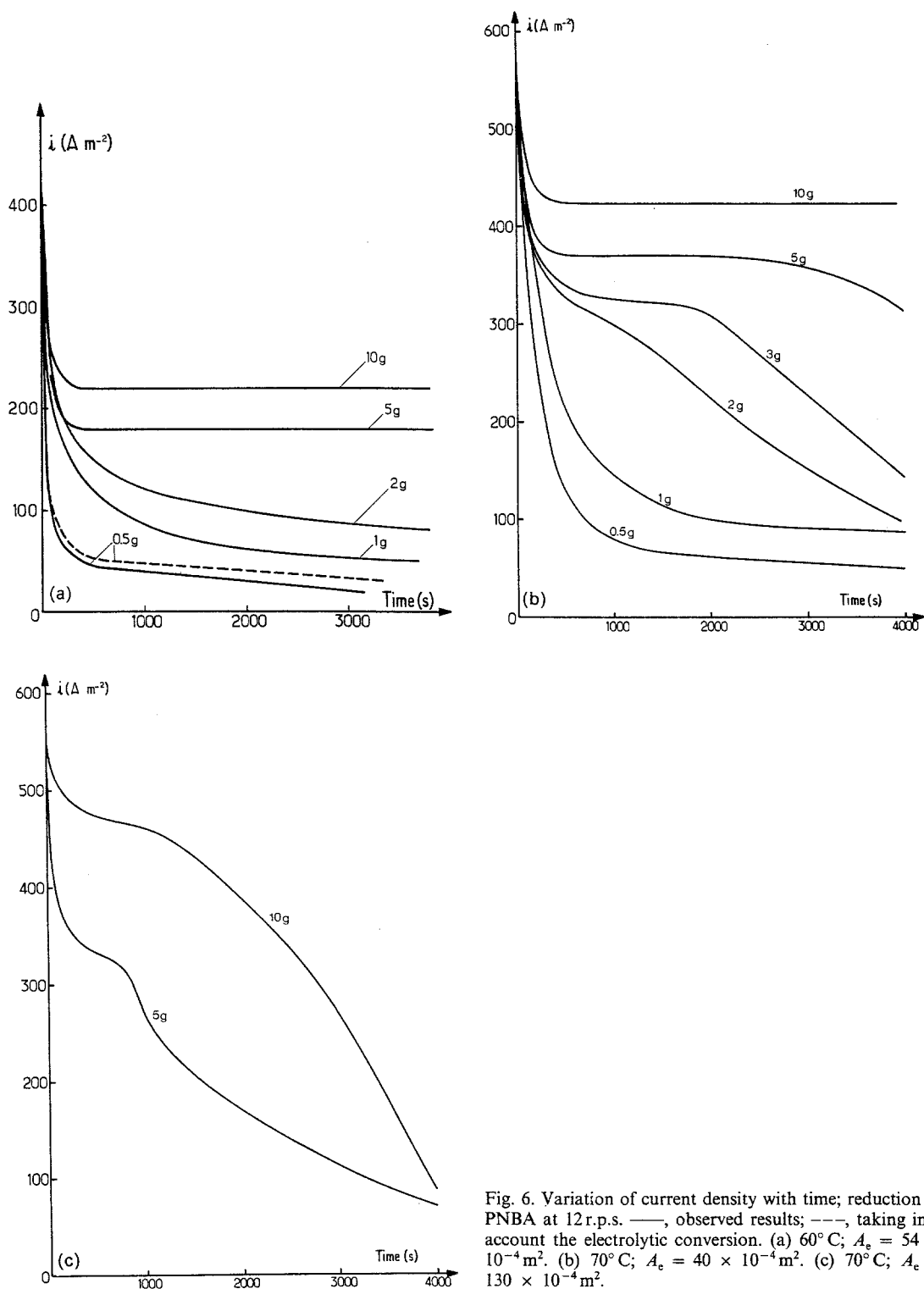


Fig. 6. Variation of current density with time; reduction of PNBA at 12 r.p.s. —, observed results; ---, taking into account the electrolytic conversion. (a) 60°C; $A_e = 54 \times 10^{-4} \text{ m}^2$. (b) 70°C; $A_e = 40 \times 10^{-4} \text{ m}^2$. (c) 70°C; $A_e = 130 \times 10^{-4} \text{ m}^2$.

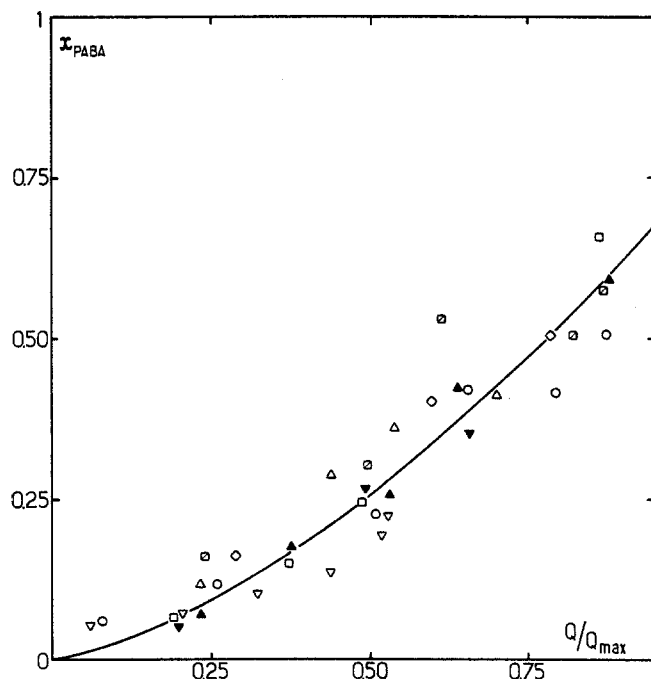


Fig. 7. Molar fraction of produced PABA versus the normalized charge passed for various amounts of PNBA; 70°C; 12 r.p.s. \diamond , \square , \boxtimes , \circ , \triangle , ∇ , $A_e = 40 \times 10^{-4} \text{ m}^2$; \blacktriangle , \blacktriangledown , $A_e = 120 \times 10^{-4} \text{ m}^2$. \diamond , $m = 1 \text{ g}$; \square , \boxtimes , $m = 2 \text{ g}$; \circ , $m = 3 \text{ g}$; \triangle , \blacktriangle , $m = 5 \text{ g}$; ∇ , \blacktriangledown , $m = 10 \text{ g}$.

account the consumption of PNBA with a faradaic yield of 100% giving proof that the decay cannot only be due to the PNBA conversion. In the case of larger quantities of substrate the evolution presents several steps, i.e. after a rapid decay the current density reaches a constant value for a certain period and then another decrease occurs.

The area of the working electrode affects the current evolution as the most important decreases are observed for the largest electrode area (Fig. 6b, c).

4.2. Production of PABA

Fig. 7 gives the experimental variations of x , mole fraction of PABA produced, versus (Q/Q_{max}) , the ratio of the charge passed to the maximal charge required for a total conversion of PNBA introduced, assuming a faradaic yield of 100%. Such a plot seems to be convenient for all experimental results obtained for various amounts of PNBA and two electrode areas.

At the beginning of the batch operation the faradaic yield of PABA produced, which is equal to the slope of the curve, is about 30–40%. Nevertheless, it is worth noting that the selectivity of the electrolytic reduction increases as the

reaction progresses. Thus total conversion of PNBA could be achieved with a yield greater than 75%.

The weak productivity in amine during the first period could be attributed to the two-step process: a transient accumulation of intermediate compounds such as hydroxylamine before a complete reduction to amine at the end of the batch operation can be invoked. Such an explanation should be confirmed by the experimental determination of the amount of hydroxylamine produced and further mathematical modelling.

5. Discussion

The observed current decay can be attributed to several factors.

(i) A chemical or electrochemical modification of the electrode surface, for instance by adsorption of the PABA produced. Another possibility is the deposition of reaction by-products which reduces the number of active sites on the electrode in the same way as inert molecules adsorb on an electrode. While much research has described the selective adsorption of specific compounds on mercury surfaces, few of them integrate this in a study relevant to electrochemical processes.

(ii) The overall conversion of solid PNBA consists of a succession of three physical processes: solubilization in the bulk, diffusion towards the electrode and electrochemical reaction. The total operation may thus be considered to be limited by the rate of PNBA solubilization.

The aim of the discussion is to propose some interpretation and to study the validity of the suggested explanations. In the present state of the art the question is posed as to whether the electrode is totally active at the beginning of the electrolysis since the acid bulk is saturated with organic substrate.

An answer to this question can be provided with the help of mass transfer analysis in the reactor. Thus current densities at ' $t \approx 0$ ', i.e. averaged quantities during the first minute, were measured for various conditions of stirring rate and temperature in the absence of a solid suspension. Assuming a faradaic yield of the reduction of 100% and a total active surface of the grid leads to corresponding values of mass transfer coefficients. Fig. 8 demonstrates that these

results expressed in dimensionless form are in a fairly good agreement with mass transfer correlations obtained for the reduction of potassium ferrocyanide. If one considers that values of the Sherwood, Reynolds and Schmidt numbers encountered here rely upon the results of experimental determination of various parameters, i.e. v , D and the grid area, it can be concluded that the electrochemical conversion of PNBA is only limited by diffusion towards the electrode in the very first instants of the operation.

The rate of solubilization of PNBA in the cathode compartment is limited by mass transfer to suspended particles. Let C^* be the saturation concentration of PNBA and C the effective concentration in the reactor. If A_s represents the total area of suspended solid and k_L the mass transfer coefficient at a particle, a mass balance in the electrochemical reactor can be expressed as follows

$$V_c dC/dt + k_d A_e C = k_L A_s (C^* - C) \quad (8)$$

and

$$i = v_e F k_d C \quad (9)$$

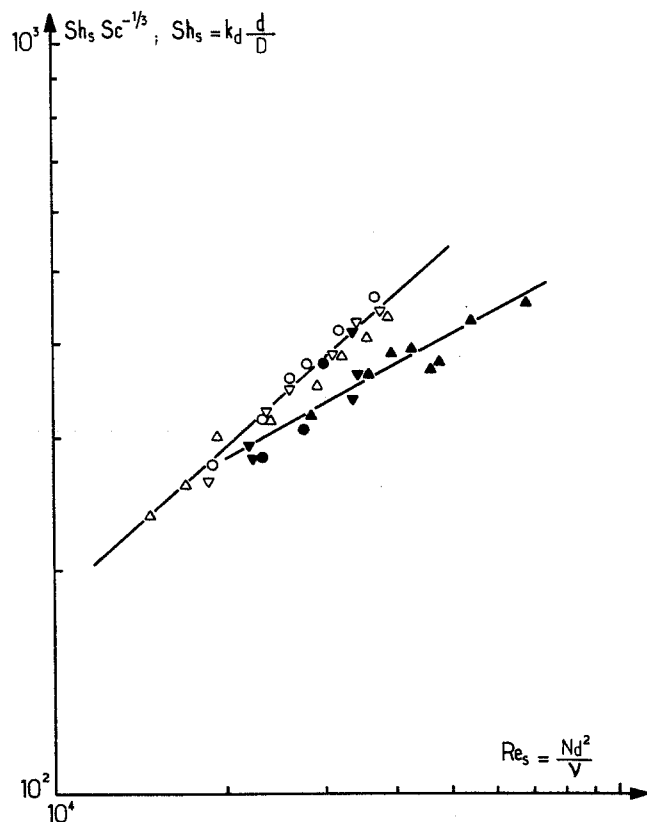


Fig. 8. Dimensionless mass transfer correlation in the reactor with two redox couples. \circ , ∇ , Δ , potassium ferricyanide (Fig. 4a); \bullet , \blacktriangledown , \blacktriangle , PNBA reduction; Sc varying from 190 to 600.

under the assumption of very fast electrochemical processes.

Introducing the interfacial areas a_e and a_s leads to

$$dC/dt + k_d a_e C = k_L a_s (C^* - C) \quad (10)$$

Limitation by the solubilization of solid particles can be effective for significant values of the concentration difference ($C^* - C$). Equation 10 shows that such a situation may be observed if the product ($k_L a_s$) is lower or of the same order of magnitude as ($k_d a_e$). First measurements of ($k_L a_s$) in the reactor used here lead us to believe that the electrolytic reduction of solid PNBA could be partly controlled by the kinetics of solubilization.

The importance of solubilization phenomena can be characterized by the dimensionless factor, α , defined as

$$\alpha = k_d a_e / (k_d a_e + k_L a_s) \quad (11)$$

For small values of α the electrolytic operation is controlled by mass transfer at the electrode. On the other hand, a α value close to unity corresponds to a PNBA reduction in an homogeneous phase. Integrating Equation 10 leads to

$$i/i^0 = 1 - \alpha + \alpha \exp(-k_d a_e t/\alpha) \quad (12)$$

where i^0 is the initial current density, for which $C = C^*$.

The theoretical variation of current density with time is plotted in Fig. 9 for similar conditions of temperature, stirring rate and electrode area as for the experimental results presented in Fig. 6b. In agreement with our experimental results the calculated current density decreases as the ratio α tends to 1, i.e. for large values of electrode area or for small amounts of suspended solid.

This simple approach, assuming a faradaic yield equal to unity, gives a satisfactory interpretation of the observed phenomena. However, numerical values of product ($k_L a_s$) are not available for the suspension used here and the results given in Figs 6b and 9 cannot be directly compared except for totally solubilized substrate ($\alpha = 1$; $m = 0.5$ g). In this case a certain discrepancy is observed between experimental and theoretical current density. This could be due to unrealistic assumptions with regards to the faradaic yield. On the other hand

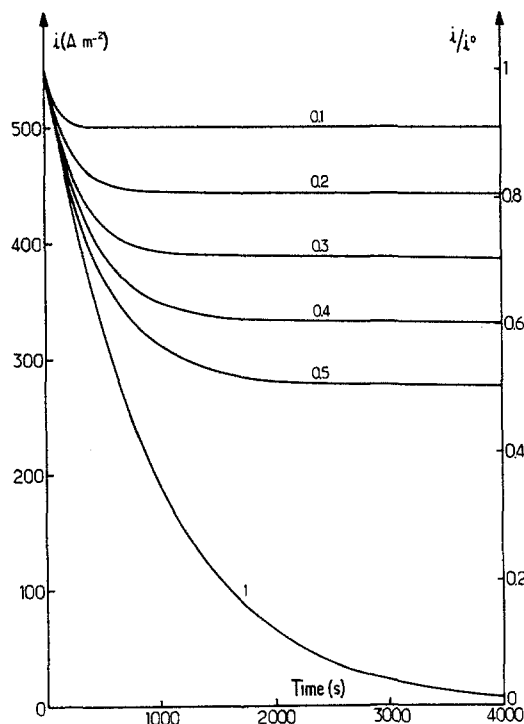


Fig. 9. Theoretical time variation of current density during the PNBA reduction for various values of α .

an alteration of the electrode surface due to the adsorption of by-products may explain this difference.

6. Conclusions

This paper presents original results on the electrochemical reduction of 4-nitrobenzoic acid into 4-aminobenzoic acid at an amalgamated copper electrode. From experimental data and by means of a chemical engineering approach, a reactor adapted to solid-liquid electrochemistry was successfully designed and tested. PABA was produced with faradaic yield close to 75% under an average current density of about 250 A m^{-2} .

Interpretation and modelling of the results is only possible through further experimental studies. Fundamental electrochemistry and organic chemistry could provide a better understanding of the electrochemical mechanism of the reduction. In addition, the effect of solid particles has to be investigated with regards to the kinetics of solubilization and the mass transfer at the electrode. This problem could be approached in a similar way as used

with liquid-liquid emulsions in electrochemical engineering [10, 11].

References

- [1] R. Kanakam, A. P. Shakunthala, S. Chidambaram, M. S. V. Pathy and H. V. K. Udupa, *Electrochim. Acta* **16** (1971) 423.
- [2] S. Chidambaram, M. S. V. Pathy and H. V. K. Udupa, *Indian J. Appl. Chem.* **34** (1971) 1.
- [3] J. Chaussard and C. Lahitte, Brevet no 81 17314, France (1981).
- [4] K. Chandra, I. Bala, H. C. Goel and M. Singh, *J. Electrochem. Soc. India* **33** (1984) 251.
- [5] S. Nagata, 'Mixing - Principles and Applications', Wiley and Sons, New York (1975).
- [6] N. Midoux and J. C. Charpentier, *Entropie* **88** (1979) 5.
- [7] A. Storck, J. F. Brodberger, D. Hutin and G. Valentin, *J. Appl. Electrochem.* **11** (1981) 723.
- [8] P. H. Calderbank and M. B. Moo Young, *Chem. Eng. Sci.* **16** (1961) 39.
- [9] A. Storck and D. Hutin, *Can. J. Chem. Eng.* **58** (1980) 92.
- [10] R. Dworak and H. Wendt, *Ber. Bunsenges. Phys. Chem.* **81** (1977) 729.
- [11] C. Furiat, G. Valentin and A. Storck, *Bull. Soc. Chim. France* **6** (1985) 1061.